Pergamon

0014-3057(95)00151-4

Eur. Polym. J. Vol. 32, No. 4, pp. 515–521, 1996
Copyright © 1996 Elsevier Science Ltd
Printed in Great Britain. All rights reserved
0014-3057/96 $15.00 + 0.00

STUDIES ON METAL COMPLEXES OF SMH RESIN

RITA MENDEZ, K. USHA, K. K. MOHAMMED YUSSUF and
V. N. SIVASANKARA PILLAI*

Department of Applied Chemistry, Cochin University of Science and Technology, Kochi 682022, India

(Received 11 January 1995; accepted in final form 14 March 1995)

Abstract—The nature of bonding in poly(styrene-co-maleic hydroxamic acid) resin complexes of Fe(III), Cu(II), Ni(II), and Co(II) was investigated using FT-i.r., electronic and EPR spectra. Ligand to metal bonding is through the hydroxamic acid–nitrogen. Fe(III), Co(II), and Ni(II) show octahedral geometry and Cu(II) shows a square planar geometry. Thermal decomposition studies by TG and DTA indicate catalysis of decomposition by the central metal atom. The activation energy for decomposition was evaluated by the Coats–Redfern equation. The SMH resin and its metal complexes show three decomposition stages above 100°C.

INTRODUCTION

In the development of metal ion-specific polymers, a detailed understanding of the coordination geometry of the polymer segment around the metal ions is important. The hydroxamic acid group is well known for its ability for form highly stable chelates with metal ions [1]. Physico-chemical methods, mainly based on spectral and magnetic properties, have been used to obtain structural information of polymer complexes. Hoek and Reedigk carried out such an investigation with the aid of electronic and EPR spectra on the metal complexes of commercially available chelating resin Chelex-100 having a styrene–divinylbenzene matrix to which iminodiaccetate groups are attached [2]. Studies on other chelating polymers such as Spheron oxime 1000-A with 8-quinolinol functional groups attached to a hydroxyethyl methacrylate matrix have been reported [3, 4]. The coordination chemistry of hydroxamic acid complexes is well documented. The work has been extended here to the complexes formed by polymer-bound hydroxamic acid with metal ions. An important feature of polymer-bound ligand coordination to the metal is the steric restriction imposed on the ligand by the polymer backbone. This becomes more prominent when the coordinating functions are on vicinal positions. The coordination geometry around the metal ion restricts coordination by vicinal dihydroxamic acid. So far no work has been reported on the coordination geometry of bound metal ions on chelating resins with hydroxamic acid functional groups at vicinal positions. Poly(styrene-co-maleichydroxamic acid) resin (SMH) provides a typical opportunity to probe the influence of the vicinal groups on the coordinating features of the complexes formed with various metal ions. In this paper we discuss the results of the studies on the SMH complexes of Cu(II), Fe(III), Co(II) and Ni(II) using electronic, EPR and Ft-i.r. spectroscopy and TG-DTG and DTA.

*Present address for correspondence: School of Environmental Studies, Cochin University of Science and Technology, Fine Arts Avenue, Kochi 682016, India.

EXPERIMENTAL PROCEDURES

Poly(styrene-co-maleichydroxamic acid) resin was prepared according to the procedure reported earlier [5]. The resin was characterized by estimating the functional group capacity, and by thermal analysis and i.r. spectroscopy. Complexes of Cu(II), Fe(III), Co(II) and Ni(II) were prepared by shaking 1 g of SMH resin (100–200 mesh ASTM) with 200 ml of the metal ion solution containing 400 mg of the metal at the pH of maximal sorption. The mixture was gently stirred for 8 hr, washed with distilled water and dried at ambient temperature in vacuum for 10 hr.

Instruments

Solid-state electronic spectra of the complexes in the region of 300–2000 nm were recorded with a Hitachi U-3410 spectrophotometer using mull technique [6]. FT-i.r. spectra in the region 500–4000 cm^{-1} were recorded using a BOMEM DA 3.16 FT-i.r. spectrophotometer. The EPR powder spectra were taken in a Varian E 109 spectrometer at room temperature.

TG-DTG and DTA thermograms were recorded on a Du Pont 990 Thermal Analyser. A dynamic dry nitrogen atmosphere at a flow rate of 50 ml min^{-1} was kept over the samples and a heating rate of 10°C min^{-1} was employed.

RESULTS AND DISCUSSION

Infrared spectra

The characteristic absorption bands of SMF resin and its Fe(III), Cu(II), Co(II) and Ni(II) complexes are given in Table 1. The frequency of N–O absorption bands in SMH resin shifts from 1085 cm^{-1} to 1074 cm^{-1} in metal complexes. This decrease is attributed to the effect of coordination of nitrogen of the hydroxamic acid group to the metal resulting in a decrease in N–O vibrational frequency. Similarly, the absorption band at 1250 cm^{-1} due to ν_{C-N} shifts to 1230 cm^{-1}, which further confirms the coordination of the nitrogen atom.

Table 1. i.r. absorption bands (cm^{-1}) of SMH resin and its metal complexes

SMH	SMH–Cu(II)	SMH–Fe(III)	SMH–Ni(II)	SMH–Co(II)	Assignment of relevant bands
3450 (b)	3450 (b)	3450 (b)	3450 (b)	3450 (b)	νOH (bound water) and NH)
1654 (s)	1708 (v.s.)	1693 (v.s)	1700 (v.s)	1703 (v)	νC—O (hydroxamic acid)
1562 (m)	1562 (sh)	1562 (sh)	1562 (sh)	1562 (sh)	νN—H
1250 (s)	1230 (s)	1230 (s)	1230 (s)	1230 (s)	νC—N
1085 (m)	1072 (m)	1072 (m)	1072 (m)	1072 (m)	νN—O
1492 (m)	1492 (m)	1496 (m)	1496 (m)	1496 (m)	νC—C (Ar)
1408 (m)	1408 (sh)	1408 (sh)	1408 (sh)	1408 (s)	νCOO^-
—	1385 (w)	1385 (w)	1385 (w)	1385 (w)	νCOO^-
702 (s)	702 (s)	702 (s)	702 (s)	702 (s)	νC—H (Ar)

b, broad; s, strong; vs, very strong; w, weak; m, medium; sh, shoulder.

A considerable increase for the carbonyl stretching frequency from 1654 cm^{-1} in uncomplexed resin to 1708 cm^{-1} and 1693 cm^{-1} is observed in the case of copper and iron complexes, respectively. Had the coordination occurred through the oxygen atom of the carbonyl group, the spectra of the complexes would have shown a decrease in the carbonyl stretching frequency. Therefore, the carbonyl group is not involved in coordination. The increase in frequency is certainly a secondary effect of the coordination through the nitrogen atom. This can be understood from the two resonance structures possible for the hydroxamic acid group.

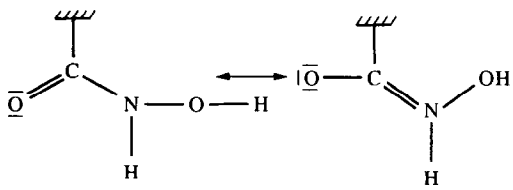

(A) (B)

The higher absorption frequency of the carboxyl group can be attributed to the contribution of resonance from (a) to the structure of the complexes. Such an increase in >C=O frequency and a decrease in —CN frequency has already been reported [7] in the case of urea complexes of Pd(II) and Pt(II) which are known to coordinate through the nitrogen atom. A band due to ν_{COO^-} is seen at 1408 cm^{-1} in the spectra of ligand and complexes, which could be due to the presence of the unconverted free carboxylic acid group. A new band is also seen at 1385 cm^{-1} in the spectra of all complexes, indicating participation of some of these carboxylic groups in coordination to the metal. The broad band at 3450 cm^{-1} due to the OH and NH stretching frequencies is observed in both complexed and uncomplexed resin spectra.

Electronic spectra

The electronic spectral data of SMH metal complexes are given in Table 2. The Fe(III) complex shows only a shoulder band at 25,400 cm^{-1}, which might be due to the charge transfer transition. The absence of d–d bands suggests that the complex has a high spin octahedral structure [8].

The bands observed for Co(II) and Ni(II) are similar to those observed in cobalt-loaded and nickel-loaded Chelex 100 resin [3, 9], in which case the coordination has been reported to be octahedral. The three bands at 8000 cm^{-1}, 13,000 cm^{-1} and 25,000 cm^{-1} for the Cu(II) complex suggest a square planar structure [10]. The high selectivity of the resin for Cu(II) compared to other metals can be explained on the basis of these observations. The donor atom of the polymer bound ligand must be flexible enough to permit an obligatory tetrahedral or square planar geometry, thus favouring more stable chelation of Cu(II) over Fe(III) [11].

EPR spectra

The EPR spectra of Fe(III), Ni(II), and Co(II) complexes are found to have many hyperfine structures, indicating that the bonding might be through the nitrogen atom.

The EPR spectra of copper complexes show one H⊥ and two H∥ maxima. In this case g∥ and g⊥ values were calculated and were found to be 2.35 and 2.08, respectively. Further, the A∥ value was found to be 140 G. Similar values have been reported [12, 13] for other chelating resins forming square planar Cu(II) complexes. Hence, these results also suggest a

Table 2. Electronic spectral data of SMH-metal complexes

Substance	Absorption maxima (cm^{-1})	Tentative assignment
SMH–Fe(II) complex	25,400	Charge transfer transition.
SMH–Co(II) complex	19,500	$^4T_{1g}(F) \rightarrow {}^4T_{1g}(P)$
	8750	$^4T_{1g}(F) \rightarrow {}^4T_{2g}$
SMH–Cu(II) complex	25,000	$^2B_{1g} \rightarrow {}^2E_{1g}$
	13,000	$^2B_{1g} \rightarrow {}^2B_{2g}$
	8000	$^2B_{1g} \rightarrow {}^2A_{1g}$
SMH–Ni complex	27,000	$^3A_{2g} \rightarrow {}^3T_{2g}$
	14,800	$^3A_{2g} \rightarrow {}^3T_{1g}(F)$
	8300	$^3A_{2g} \rightarrow {}^3T_{1g}(P)$

Table 3. Thermal decomposition data of SMH resin and its metal complexes

Substance	Peak temperature in DTA (°C)	Temperature range in DTA (°C)	Peak temperature in DTG (°C)	Temperature range in DTG (°C)	Stage of decomposition	Loss from TG (%)
1	2	3	4	5	6	7
SMH resin	70 endo (w)	50–90	60	30–80	I	20.00
	320 exo (m) (sh)	260–360	320	260–360	II	13.79
	385 exo (m) (sh)	360–480	385	360–480	III	16.32
	755 exo (vs)	700–820	740	670–770	IV	23.40
SMH–Fe complex	70 endo (w)	60–90	60	30–90	I	7.90
	265 endo (w)	200–285	270	190–290	II	10.88
	310 exo (w)	285–330	310	290–335	III	10.00
	450 exo (s)	330–620	435	335–470	IV	58.14
SMH–Co complex	70 endo (w)	50–90	60	40–90	I	10.00
	330 exo (w)	275–350	340	275–345	II	12.64
	385 exo (w)	350–400	335	345–395	III	15.94
	410 exo (s)	400–560	410	395–510	IV	55.50
SMH–Cu complex	70 endo (w)	50–90	60	40–90	I	10.00
	250 exo (m)	210–280	245	210–275	II	12.38
	310 exo (m)	280–370	305	275–370	III	18.56
	485 exo (s)	370–600	465	360–500	IV	40.46
SMH–Ni complex	70 endo (vw)	50–90	60	40–90	I	14.00
	335 exo (vw)	295–350	335	300–345	II	14.70
	365 exo (w)	350–375	365	345–370	III	14.00
	395 exo (vs)	375–435	395	370–435	IV	40.30

s, strong; vs, very strong; w, weak; m, medium; sh, sharp; vw, very weak; endo, endothermic; exo, exothermic.

square planar coordination for the SMH–Cu(II) complex.

Thermal behaviour

The values of the DTG peak temperatures and temperature of completion for each stage of decomposition together with mass loss data are presented in Table 3. The TG, DTG, and DTA curves for the SMH resin and its complexes are given in Fig. 1.1 to 1.5. There are four stages of decomposition for the SMH resin as well as its metal complexes. All the compounds dried at ambient temperatures are seen to lose their mass, even from 40°C for which the corresponding DTG peak is around 60°C and is paralleled by a weak endothermic DTA peak around 70°C. The mass loss at this stage is due to the removal of interstitially absorbed water and is also evidenced by a broad band in the region 3060 cm^{-1} in the i.r. spectra.

The mass loss corresponding to the other three stages might be due either to the decomposition of the functional groups or to the degradation of the poly-

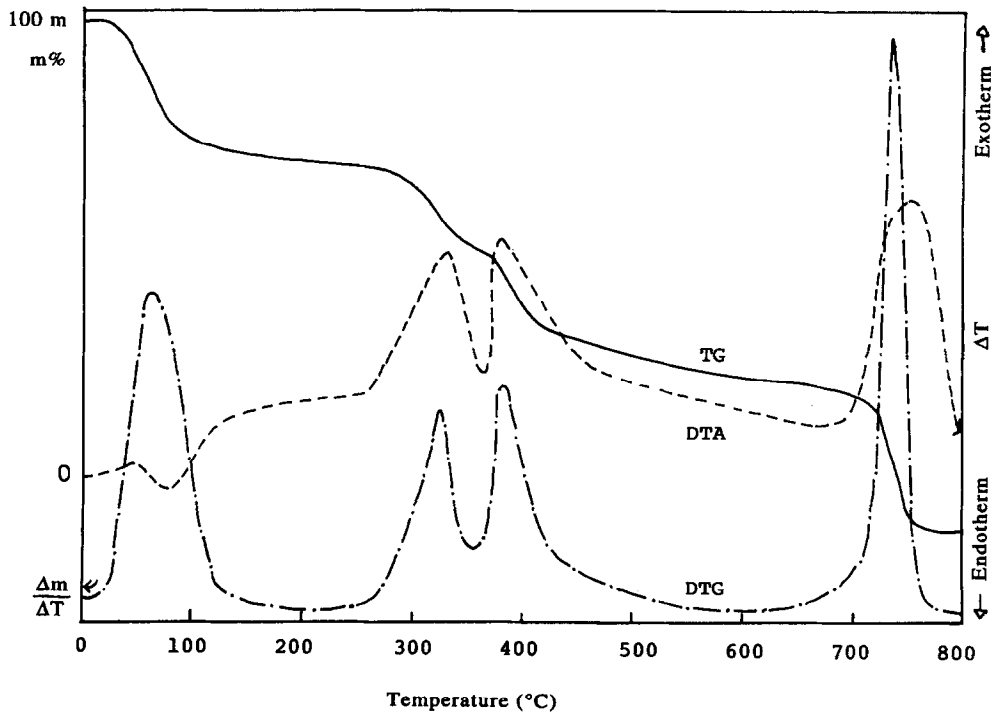

Fig. 1. TG, DTG and DTA of SMH resin. Heating rate 10°C min^{-1}, N_2 flow rate 50 ml min^{-1}.

Table 4. Kinetic parameters for the thermal decomposition of SMH resin and its metal complexes

Substance	Stage of decomposition	Order (n)	E_a (kJ mol^{-1})	A (s^{-1})	ΔS (kJ mol^{-1} K^{-1})	r
SMH resin	II	1.17	132.69	2.59×10^{9}	−70.49	0.9945
	III	3.18	329.90	1.80×10^{24}	212.88	0.9885
	IV	0.764	603.63	12.124×10^{29}	320.93	0.9929
SMH–Fe complex	II	0.08	66.90	8.20×10^{3}	−174.99	0.9929
	III	1.431	257.52	1.164×10^{21}	152.83	0.9821
	IV	1.03	130.27	0.389×10^{8}	−106.81	0.9914
SMH–Co complex	II	0.991	175.25	1.539×10^{13}	1.55	0.9439
	III	1.38	298.62	1.96×10^{32}	175.33	0.9959
	IV	1.47	199.27	2.626×10^{12}	−33.50	0.9818
SMH–Cu complex	II	1.62	185.75	5.418×10^{16}	70.86	0.9949
	III	2.27	180.93	1.217×10^{14}	19.23	0.9941
	IV	1.84	149.62	4.365×10^{8}	−87.06	0.9809
SMH–Ni complex	II	1.294	274.92	0.6889×10^{22}	167.26	0.9981
	III	0.142	82.49	2.70×10^{17}	237.49	0.9986
	IV	1.01	212.18	2.08×10^{14}	22.49	0.9982

mer. All the DTG peaks corresponding to these stages have complementary DTA peaks. The decomposition reactions are generally expected to be endothermic. The exothermicity of the DTA peaks in the present cases might be due to oligomerization reactions of the products of decomposition [14].

The DTG peak temperature for the final decomposition stage has been lowered from 740°C for SMH resin to 400–450°C for its metal complexes. This might be due to the catalytic effect of the metal ions on the decomposition of SMH resins.

The thermolysis of SMH in a nitrogen atmosphere leaves a residue of 14.7%, whereas the metal complexes given only lower quantities of the residue [Fe(III), 8.6%; Co(II), 10.0%; Cu(II), 13.90% and Ni(II), 12.0%]. This also lends evidence to the catalytic activity of the metal ion in bringing about a more exhaustive degradation of the polymer.

Decomposition kinetics

The kinetic parameters for the different stages of decomposition have been calculated using the Coats–Redfern equation [15] and are presented in Table 4. The final form of the Coats–Redfern equation is

$$\log g(\alpha)/T^2 = \log \frac{AR}{\phi E_a} - \frac{E_a}{2.303RT},$$

where α is the degree of conversion, ϕ the heating rate, A the pre-exponential factor, E_a the activation energy, T the temperature in Kelvin, R the gas constant, and g the function of α, where

$$g(\alpha) = 1 - (i - \alpha)^{1-n}/(1 - n)$$

when $n \neq 1$, and

$$g(\alpha) = -\ln(1 - \alpha)$$

when $n = 1$.

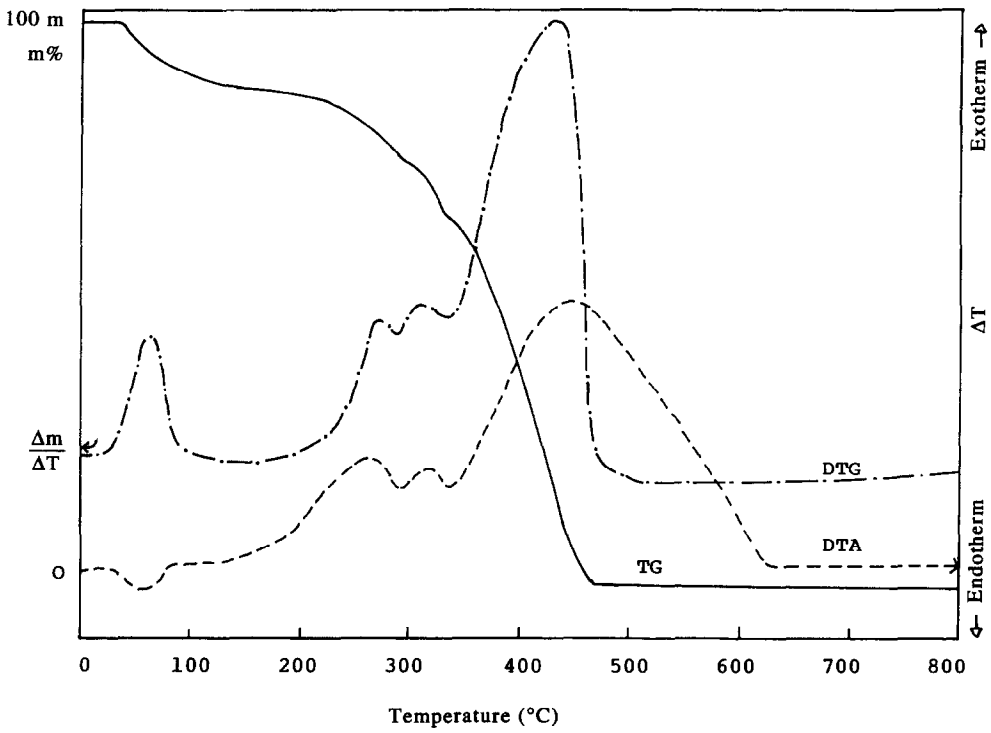

Fig. 2. TG, DTG and DTA of SMH–Fe(III) complex. Heating rate 10°C min^{-1}, N_2 flow rate 50 ml min^{-1}.

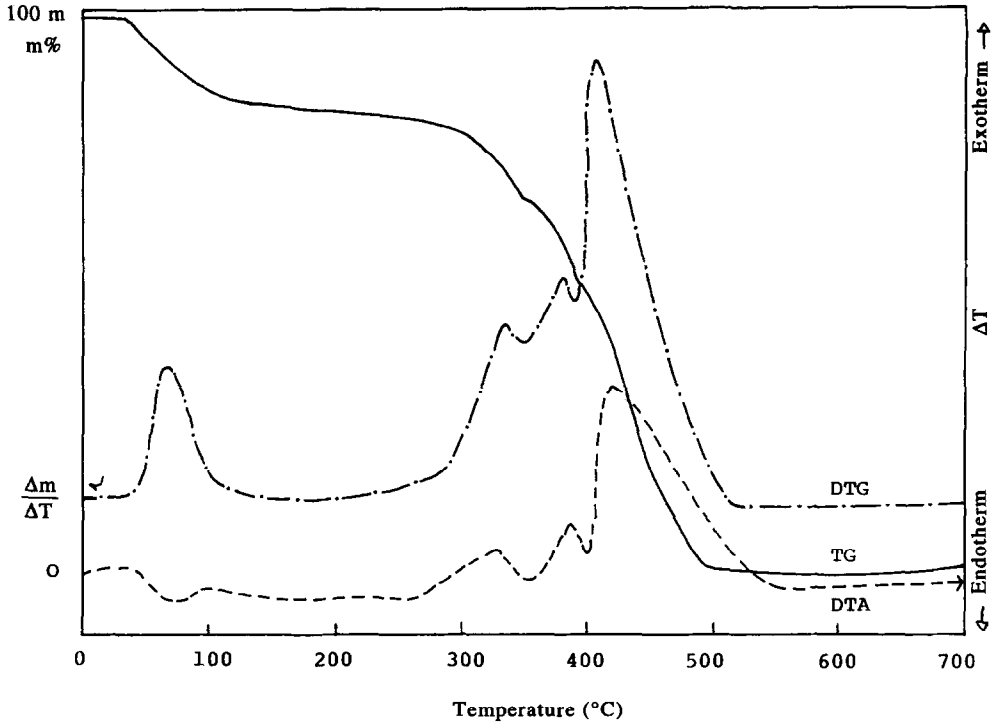

Fig. 3. TG, DTG and DTA of SMH–Co(II) complex. Heating rate 10°C min^{-1}, N_2 flow rate 50 ml min^{-1}.

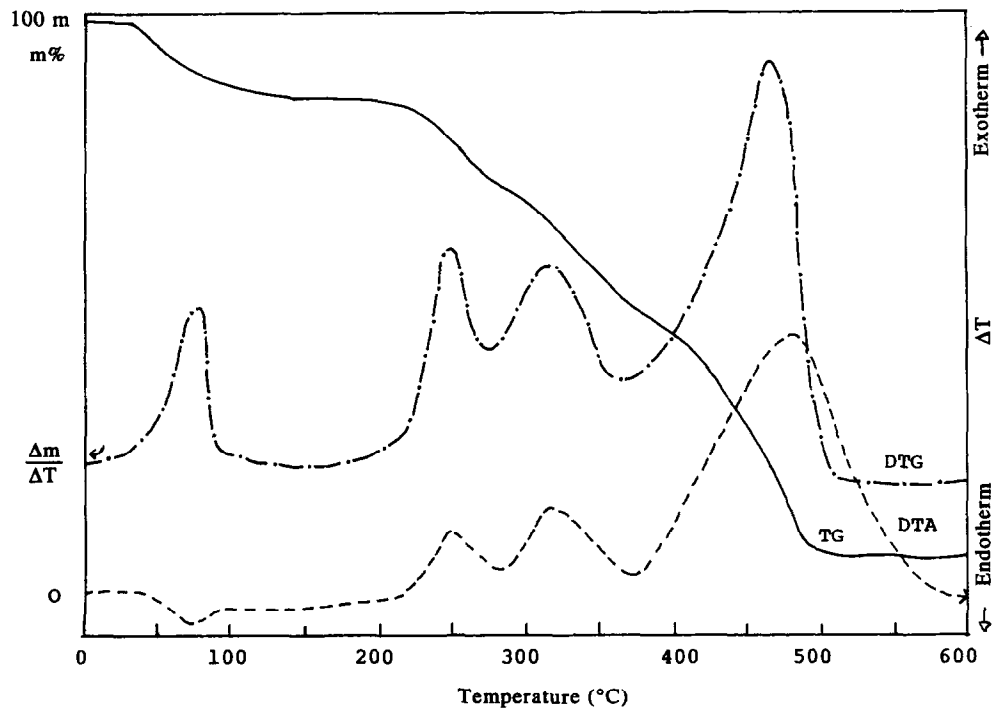

Fig. 4. TG, DTG and DTA of SMH–Cu(II) complex. Heating rate 10°C min^{-1}, N_2 flow rate 50 ml min^{-1}.

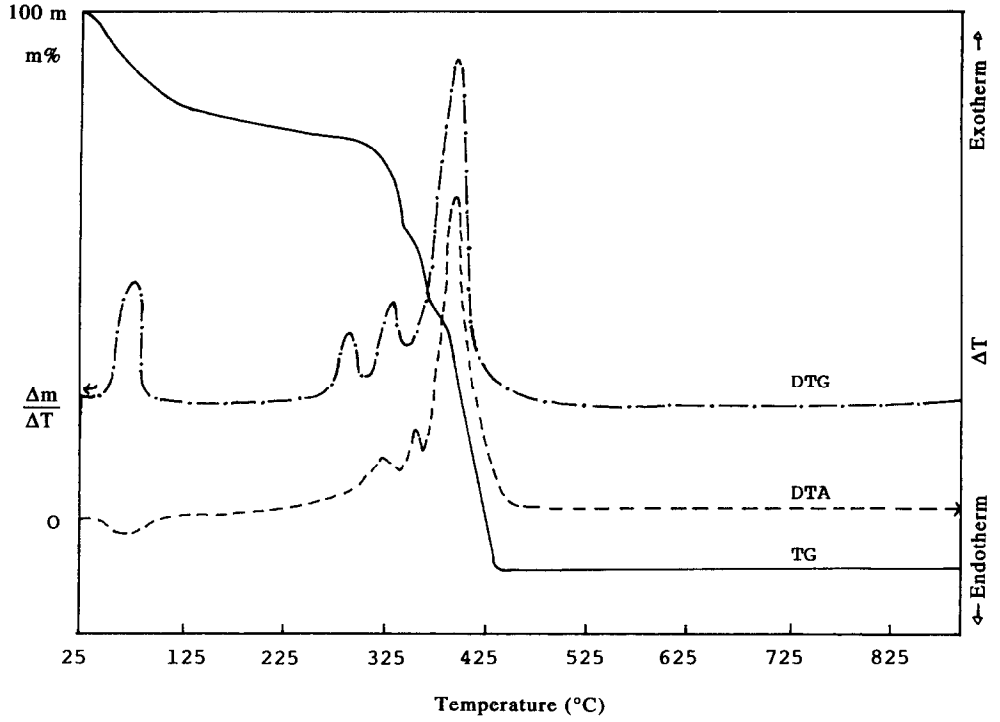

Fig. 5. TG, DTG and DTA of SMH–Ni(II) complex. Heating rate 10°C min^{-1}, N_2 flow rate 50 ml min^{-1}.

A plot of $\log g(\alpha)/T^2$ against $1/T$ is linear. The value of E_a is obtained from the slope, and the intercept gives A. The entropy of activation ΔS is calculated using the relation $A(=kT/h)e^{\Delta S/R}$ where k is the Boltzmann constant, and h is the Planck's constant.

The correlation coefficient (r) is in the range of 0.9900 to 0.9986 for most of the data indicating a perfect fit. The parameters E_a and ΔS are employed for the comparison of the decomposition process [16] of similar compounds.

A comparison of E_a for the SMH resin with those of the SMH–metal complexes for the second stage of decomposition shows that E_a increases considerably for the Co(II), Ni(II) and Cu(II) complexes, indicating a lower rate of decomposition at this stage. However, in the case of the Fe(III) complex the E_a value decreases, indicating a faster rate of decomposition. The ΔS value for the SMH resin is negative, indicating a highly ordered activated state. In the Co(II), Cu(II) and Ni(II) complexes, ΔS has positive values, indicating that the activated complexes are less ordered for this stage. For the Fe(II) complex ΔS has become more negative, which may be due either to the chemisorption of the decomposition products [17] or to the reduction of Fe(III) to Fe(II).

The E_a and ΔS values for the third stage of decomposition are lower for the metal complexes than for the resin, indicating faster decomposition of the complexes at this stage. This again can be attributed to the catalytic effect of the metal species formed during decomposition.

For the last stage of decomposition the catalytic activity of the metal ions is the most pronounced. The ΔS values for the Cu(II), Co(II) and Fe(III) complexes are negative, indicating a highly ordered state. The large decreases in E_a values for the metal complexes shows that the catalytic effect of the metal ions is in the order Fe(III) > Co(II) > Cu(II) > Ni(II).

Acknowledgement—RM thanks CSIR, Government of India, for financial support.

REFERENCES

1. A. Winston and G. R. Mchaghlin. *J. Polym. Sci.* **14,** 2155 (1976).
2. M. Kaneko and E. Tsuchida. *Macromol. Rev.* **16,** 522 (1981).
3. P. J. Hoek and J. Reedijk. *J. Inorg. Nucl. Chem.* **41,** 401 (1979).
4. P. J. Hoek and J. Reedijk. *J. Inorg. Nucl. Chem.* **47,** 1759 (1980).
5. R. Mendez and V. N. S. Pillai. *Talanta* **37,** 591 (1990).
6. G. Dyer, J. G. Hartley and L. M. Venanzi. *J. Chem. Soc.* 1293 (1965).
7. R. S. Drago. *Physical Methods in Chemistry*, p. 176. Saunders, Philadelphia (1969).
8. R. S. Drago. *Physical Methods in Chemistry*, p. 392. Saunders, Philadelphia (1969).
9. F. A. Cotton. *Coord. Chem. Rev.* **8,** 184 (1972).
10. A. B. P. Lever. *Inorganic Electronic Spectroscopy*, 2nd edn. New York (1984).
11. S. K. Sahni and J. Reedijk. *Coord. Chem. Rev.* **59,** 29 (1984).
12. H. Nishide, J. Deguchi and E. Tsuchida. *J. Polym. Sci. Polym. Chem.* **15,** 3023 (1977).
13. H. Nishide, N. Shimidzu and E. Tsuchida. *J. Appl. Polym. Sci.* **27,** 4161 (1982).

14. N. Grassie. *Developments in Polymer Degradation*, p. 140. Applied Science Publishers, London, England (1977).
15. A. W. Coats and J. P. Redfern. *Nature* **68**, 201 (1964).
16. G. N. Natu, S. K. Kulkarni and P. S. Dhar. *J. Therm. Anal.* **23**, 101 (1982).
17. P. M. Madhusudhanan, K. K. M. Yusuff and C. G. R. Nair. *J. Therm. Anal.* **8**, (1975).